Site classification and Vs30 estimation of free-field TSMIP stations using the logging data of EGDT

Chun-Hsiang Kuo [a,*], Kuo-Liang Wen [a,b], Hung-Hao Hsieh [a], Che-Min Lin [a], Tao-Ming Chang [a], Kai-Wen Kuo [c]

[a] National Center for Research on Earthquake Engineering, Taipei, Taiwan
[b] Institute of Geophysics, National Central University, Taoyuan, Taiwan
[c] Seismology Center, Central Weather Bureau, Taipei, Taiwan

ARTICLE INFO

ABSTRACT

The Engineering Geological Database for TSMIP (EGDT), the Taiwan Strong Motion Instrumentation Program, has been under construction by the National Center for Research on Earthquake Engineering and the Central Weather Bureau in Taiwan since 2000. Site characterization, comprising surface investigations and logging measurements, was carried out throughout the project. We provide a set of specifications and a description to help users understand the subject matter of the database. EGDT contains 469 surveyed stations, 439 of which were drilled and the logging measurements completed. Of these, 385 had logging data reaching at least 30 m, and we used these to examine and determine the most accurate extrapolation of Vs30 (the average S-wave velocity of the top 30 m of strata) for the other 54 stations with velocity profiles less than 30 m. The chosen method assumed that the bottom velocity is identical from the actual depth of the hole to a distance of 30 m, that is, the Bottom Constant Velocity (BCV) method. In order to utilize other existing boreholes which have only N values but no velocities in the future, the empirical S-wave velocity equations for seven different regions and the whole of Taiwan were evaluated by a multivariable analysis. Henceforth, for those existing boreholes which have an N profile less than 30 m, the S-wave velocity profile can first be calculated by empirical S-wave velocity equations, and then Vs30 can be estimated by reliable extrapolation. Some other studies of site classifications of TSMIP stations were compared with our results to demonstrate the necessity of reclassification. Ultimately, the Vs30 values of the 439 drilled free-field TSMIP stations were derived and the new site classification was achieved according to the Vs30-based provisions of the National Earthquake Hazards Reduction Program.

© 2012 Elsevier B.V. All rights reserved.

1. Introduction

The soft deposits overlaid on the hard bedrock are believed to increase seismic amplification and cause increased damage during a large earthquake. This is the so-called site effect, a very important issue in strong ground motion studies. The different characteristics of near-surface layers cause various effects at sites. The so-called Vs30 (the average S-wave velocity of the top 30 m of strata) is recommended as a momentous index for defining the local geological conditions for site classification in recent building codes (e.g., Dobry et al., 2000; BSSC, 2001). The Vs30-based National Earthquake Hazard Reduction Program (NEHRP) provision classes are listed in Table 1. Because the strong ground motion sequences recorded at Chi-Chi, Taiwan, are also included in the Pacific Earthquake Engineering Research Center (PEER) database, the exact site classification, as

well as the Vs30 values of free-field TSMIP stations, is one of the essential issues for the Next Generation Attenuation (NGA) ground motion modeling project (e.g., Chiou et al., 2008; Power et al., 2008).

The Taiwan Strong Motion Instrumentation Program (TSMIP) has been carried out by the Central Weather Bureau (CWB) from 1991 to collect high-quality instrumental recordings of strong ground motions caused by earthquakes. The program comprises free-field stations and building arrays. Most of the stations were installed in the metropolitan districts of Taiwan for earthquake hazard reduction. This data is certainly useful for understanding earthquake source mechanisms, improving seismic design of buildings, and studying seismic wave propagation (including local site effects). About 700 free-field stations have been installed and are presently operating throughout Taiwan. In order to use the collected strong motion recordings more effectively and precisely, the National Center for Research on Earthquake Engineering (NCREE) and the CWB commenced a free-field strong motion drilling project to construct the Engineering Geological Database for TSMIP (EGDT) in 2000. A total of 469 free-field strong motion stations had been surveyed by 2010, and 439 of these were

---

Table 1
Site classification scheme in terms of Vs30, according to NEHRP provisions and geological sketches.

Classification	Definition of Vs30 (m/s)	Geological sketch
A	Vs30 > 1500	Hard rock
B	1500 ≥ Vs30 > 760	Firm to hard rock
C	760 ≥ Vs30 > 360	Dense soil and soft rock
D	360 ≥ Vs30 ≥ 180	Stiff soil
E	180 > Vs30	Soft soil

drilled and their seismic velocities measured by a suspension PS-logger system. Site classification and Vs30 values for all of the drilled stations are now available via the EGDT website (http://egdt.ncree.org.tw/). Detailed logging data can also be obtained from the website for free. As a summary of the description of the EGDT must be made available for people who want to use it, it is therefore introduced in the present study.

Lee et al. (2001) studied surface geology, response spectra, and horizontal to vertical spectral ratios of earthquakes to classify 708 sites of free-field strong motion stations into four categories, i.e., classes B, C, D, and E. Huang et al. (2007) calculated the Vs30 of 87 free-field strong motion stations in central Taiwan using logging data, and 85 of the 87 sites were also included in Lee's results. However, 65 of the 85 sites reclassified by Huang et al. (2007) based on Vs30 criteria were different from the previous results of Lee. Phung et al. (2006) used the response spectra of 87 stations with known site conditions to classify 333 other strong motion stations as soil and rock sites. Lee and Tsai (2008) revised the former classification (Lee et al., 2001) and mapped Vs30 for the whole of Taiwan by a geo-statistical scheme using logging data of the EGDT at 257 strong motion stations and N values of another database at 4885 engineering boreholes. Kuo et al. (2011) studied the free-field TSMIP stations in Taipei and Ilan using available logging data and pointed out considerable discrepancies between their results and those of Lee and Tsai (2008); 35 of the 110 stations were reclassified as a result. In addition, the Vs30 was estimated by a reliable extrapolation for the 16 strong motion stations with velocity profiles less than 30 m. It should be noted that the logging data used by the above studies (Huang et al., 2007; Lee and Tsai, 2008; Kuo et al., 2011), except for the 4885 engineering boreholes, are all from the EGDT. Obviously, many stations of the widely used site classification (Lee et al., 2001) were misclassified; even the improved result (Lee and Tsai, 2008) that used parts of the EGDT data is not entirely dependable. Since we have more logging data in EGDT, all of the data obtained up to and including 2010 were employed in this study, as well as an extrapolation method to categorize the drilled free-field TSMIP stations throughout Taiwan.

Considering the general problem that many velocity profiles of boreholes which were drilled before did not reach 30 m, Kuo et al. (2011) examined three common extrapolations and proposed that the BCV is the most accurate method in northeastern Taiwan. The present study also examined and adopted the accurate extrapolation for the 54 stations with velocity profiles less than 30 m in the EGDT. Furthermore, we evaluated empirical S-wave velocity equations for seven regions and the whole of Taiwan to make the calculation of S-wave velocity profiles more efficient by using existing N profiles at a certain site. Hereafter, the significant Vs30 can be assessed without additional expense, based on the idea of first calculating S-wave velocity profiles by empirical equations and then estimating Vs30 by a reliable extrapolation for those boreholes with N profiles less than 30 m.

2. Engineering Geological Database for TSMIP (EGDT)

Taiwan Island was created by the collision of the Philippine Sea Plate and the Eurasian Plate. The rate of subduction is currently about 80 mm/yr. The collision created a four-kilometer-high mountain belt and there is a high uplift rate of 5–7 mm/yr in the marine terrace (Liew et al., 1993), as well as high seismicity in and around the island. As well, Taiwan has one of the highest erosion rates in the world (Koppes and Montgomery, 2009). This is why the geology, topography, and seismicity are so varied and complex in this 36,000 km² island. After the destructive Chi-Chi earthquake, it was considered necessary to understand the variable geological conditions at strong motion stations, so that the critical site effect might be assessed. This work is going to be an important reference material for reducing the hazards of potential future earthquakes.

In its first year, 2000, the survey focused on the mutual stations of TSMIP and the Taiwan Rapid Earthquake Information Release System. The Resolution of Site Response Issues from the Northridge Earthquake (ROSRINE) utilized their methodology and experience to assist NCREE in their efforts to characterize strong motion sites with a collaborative project in 2001, and a total of 60 stations situated in the Western Plain were surveyed in the same year. Consequently, the major procedures of site characterization in the EGDT were the same as those of ROSRINE. The number of surveyed stations reached a total of 469 by 2010, and comprised over 65% of the free-field TSMIP network (Fig. 1). Of these, 439 stations were drilled, so that detailed logging data was available at those stations; for the other 30 stations, to which the equipment could not be transported or where the landowner declined the request to drill, only photos and plan view drawings were included. However, these photos and plan view drawings can be consulted when researchers are confused by unusual seismic records. For example, Wen et al. (2008) examined the local site effect at the former station of TAP056. The photos and
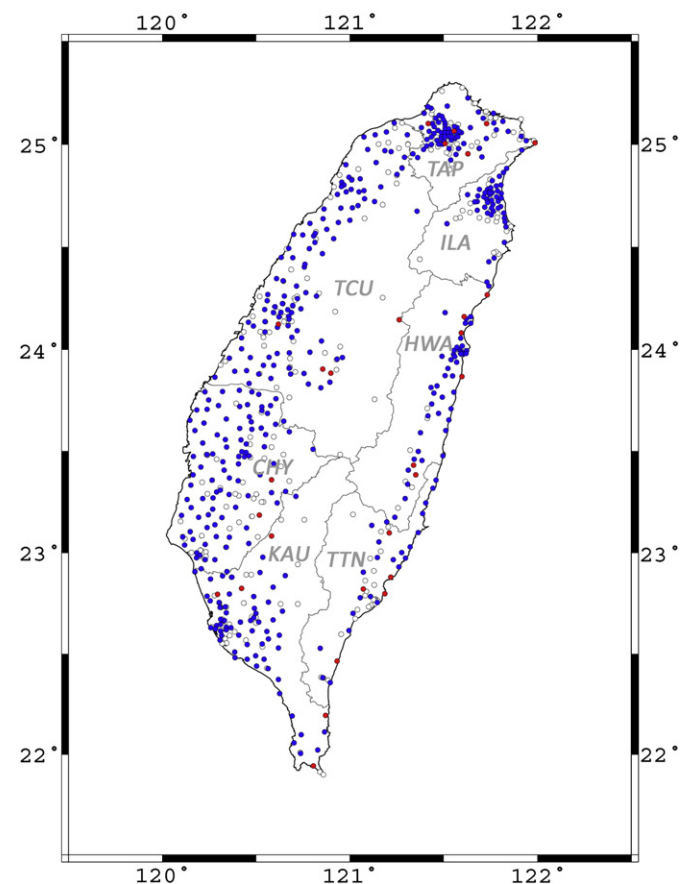
Fig. 1. The distribution of free-field TSMIP stations and zones on Taiwan Island. The blue circles are drilled stations, the red circles are surveyed stations not drilled, and open circles are stations not yet surveyed.

plan view drawings showed that the station was located at the edge of a man-made grass plot on a slope. This helped them to focus on the key aspects of the subject and work out the appropriate field survey to verify it. In the following, we will describe the methods of the drilling project, which might help users to understand the database and might provide a significant reference material for other drilling projects in the future.

Generally, a completed site characterization comprises surface investigations and logging measurements; the 30 stations without drilling therefore have no logging measurements. The surface investigations include station and borehole positioning, plan view drawings and descriptions, photography of the surrounding environment, and marking positions on aerial photographs. The positioning of stations and boreholes was performed using GPS, and provided coordinates in both TWD67 and TWD97 systems, although the distance of a borehole from a station was stipulated to be less than 3 m. Otherwise, the EGDT provided very complete and detailed high quality logging data, obtained by precise measurements in accordance with the criteria of the American Society for Testing and Materials (ASTM) (Sino Geotechnology, Inc., 2002-2010). Cores of strata were sampled, except for soils, and were then aligned to be photographed; stratigraphic columns and descriptions were also made.

An *in situ* Standard Penetration Test (SPT) was made every 1.5 m (every 3 to 5 m for gravel layers) or at the depth of notable discontinuity during the drilling. A hammer of 140 pounds was allowed to fall freely on a split tube sampler from a distance of 30 in. in each blow. The sampler was driven through three 6-inch (15.24 cm) layers. The number of blows of the sampler passing through the first, second, and third 6-inch layers are called N1, N2, and N3, respectively. The N-value is defined as the sum of N2 and N3, and the depth of the test is defined as the depth of the top of the first 6-inch layer. Additionally, the maximum number of blows of each 6-inch layer is limited to 50. An automatic system for letting the hammer fall was used during the procedure to avoid the variations which might result from a human agent. The disturbed soil samples obtained were analyzed in a laboratory certified by the Taiwan Accreditation Foundation to derive the physical characteristics of the soils, such as the grain-size distribution curve, uniformity coefficient, coefficient of gradation, void ratio, water content, specific gravity, unit weight, liquid limit, and plasticity index. The soils were classified on the basis of the Unified Soil Classification System (USCS).

Subsequently, P- and S-wave velocities were measured using a Suspension PS Logger system (OYO corporation, 1999, 2000, 2002). The boreholes were cased in 2.5-inch PVC pipes and the gap between the pipe and the hole was grouted in advance to ensure that the produced seismic waves could propagate through the layers. The sampling rate can be set from 2.5 to 200 μs and the data lengths can be chosen from 1024 or 2048 words according to the condition of the strata. In general, the frequency of the velocity measurement is every 0.5 m, except for several drilled in the first and second years, at which the frequency was 1 m per measurement. Depth sequences of P- and S-waves were plotted to help in the determination of travel times at adjacent depths. The Suspension PS Logger system has two sensors at a fixed distance of 1 m, and a source was integrated together with the sensors in a tube. This enabled continuous measurements and velocities at various depths by the system. The produced P- and S-waves were received by two sensors, for which the middle point was taken as the depth of a measurement; thus the first arrivals of the seismic waves were identified, and then the P- and S-wave velocities could be calculated (Fig. 2) by the equation:

$$Vp(d) = 1/(t_{p1} - t_{p2}), Vs(d) = 1/(t_{s1} - t_{s2}). \quad (1)$$

The $Vp(d)$ and $Vs(d)$ are the P- and S-wave velocities at a depth of d, t_{p1} and t_{s1} are the arrival times of the upper receivers, and t_{p2} and t_{s2} are the arrival times of the lower receivers. The drilled depth of the project was stipulated to be at least 35 m in the plans after 2006 to ensure that Vs30 could be measured. Unfortunately, several velocity profiles were still less than 30 m after 2006, due to boreholes collapsing. In addition, 22 boreholes were drilled over 50 m, and the deepest one was 150 m at TCU138.

The basic data we provide in the EGDT now includes coordinates, strata description, results of the soil physical property tests, P- and S-wave velocities, SPT-N values, plan views and photos; others, like grain size curves, depth sequences, aerial photographs, etc., are not provided at this stage.

3. Extrapolations of Vs30

It is a worldwide issue that many velocity profiles of drilled boreholes did not reach the required 30 m, and that 54 stations in the
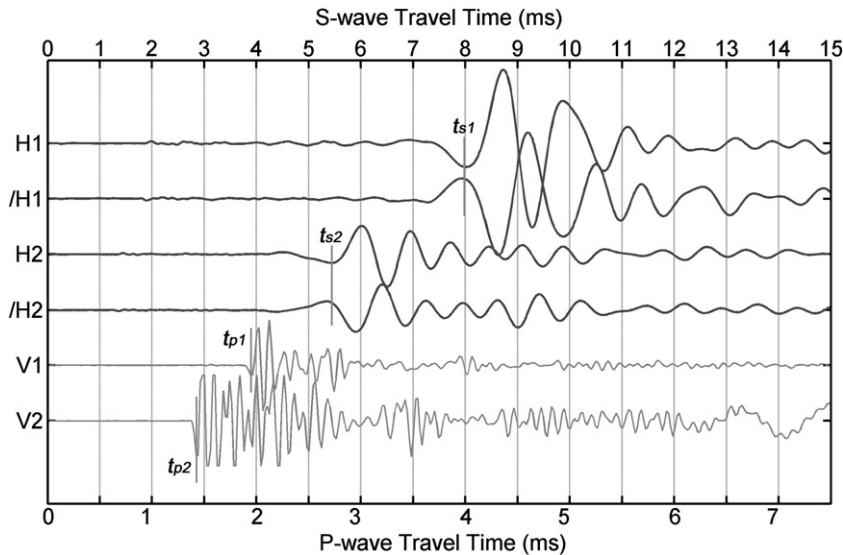

Fig. 2. Illustration of arrival times of a Suspension PS-logging measurement, where: V1 and V2 are the time histories recorded by two receivers in the vertical component; H1 and H2 are those in a horizontal component; /H1 and /H2 are those in the perpendicular horizontal component; t_{p1} and t_{p2} indicate the arrival times of the P-wave; and t_{s1} and t_{s2} indicate those of the S-wave.
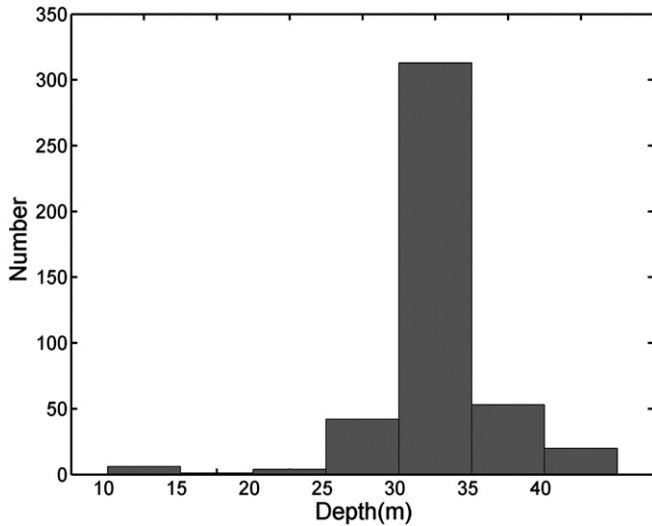
Fig. 3. Histogram of depths of the 439 drilled stations in the EGDT. Those deeper than 40 m are all plotted in the same column. The numbers of each depth interval are 6, 1, 4, 43, 312, 53, and 20 from left to right.

EGDT are shallow as well. Fig. 3 shows a histogram of the depths of the velocity profiles at the 439 drilled stations of the EGDT. Of these, 385 were deeper than 30 m; those deeper than 40 m are all plotted in the same column. The numbers of those less than 30 m were 6, 1, 4, and 43 at the depths of 10–15, 15–20, 20–25, and 25–30 m, respectively. In fact, not only site classification but also the values of Vs30 became crucial for strong ground motion predictions (e.g., Campbell and Bozorgnia, 2008; Chiou and Youngs, 2008). If the Vs30s of the profiles which were less than 30 m are to be calculated, we must devise an exact extrapolation. Boore (2004) found numerous measurements of near-surface S-wave velocity profiles that did not arrive at the required 30 m. For example, those of K-NET stations in Japan are between 10 and 20 m; more than half of the boreholes (142 of 277) in California in a recent compilation (Boore, 2003) are smaller than 30 m, and 193 of 202 seismic cone penetrometer measurements in the Oakland–Alameda area of California (Holzer et al., 2002, 2005) are less than 30 m. Therefore, plots of log Vs30 against log Vs(d) for a series of assumed depths d were found by fitting straight lines to velocity profiles with actual depths reaching at least 30 m. Here, Vs(d) is the time-averaged velocity from the surface to a depth of d. A power-law relation between Vs30 and Vs(d) was assumed and the equation was given as:

$$\log \mathrm{Vs30} = a + b\log \mathrm{Vs}(d) \tag{2}$$
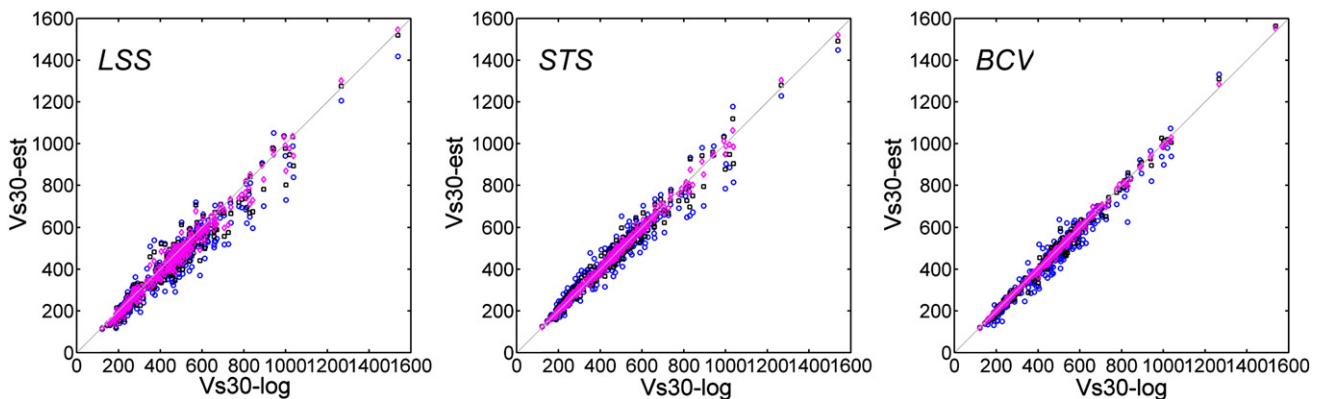
The coefficients (a, b) were obtained at different depths (10 to 28 m). A least-square method that assumed that the S-wave travel time increased with depth in a power-law relation was implemented to estimate Vs30 (Boore and Joyner, 1997; Huang et al., 2007). In other cases, a simple method that assumed that the deepest velocity is a constant from the actual depth of the hole to a distance of 30 m was adopted. The three extrapolations outlined above were named statistical extrapolation (STS), least-square fitting of a single station (LSS), and bottom constant velocity (BCV) by Kuo et al. (2011). The accuracies were assessed by using parts of the EGDT. As a result, the BCV was proposed to be the optimum extrapolation in Taipei and Ilan.

Fig. 4 illustrates the estimated Vs30 (y-axis) obtained by the extrapolations versus the measured Vs30 (x-axis) by PS-logging of the 385 drilled stations for which the velocity profiles extend to at least 30 m. The cases of the three assumed depths of 15, 20, and 25 m are represented as blue circles, black squares, and magenta diamonds, respectively. The discrepancies of all extrapolations decrease as the assumed depth increases. It is typical of an extrapolation that, when more known data is given, more accurate results are estimated. We further quantified the errors of the extrapolations by defining an error percentage (Err%):

$$\mathrm{Err\%} = \frac{\sum |V_{rel} - V_{est}| / V_{rel}}{n} \times 100\%. \tag{3}$$

Where V_{rel} is the measured S-wave velocity, V_{est} is the S-wave velocity estimated by extrapolation, and n is the number of data points. The calculated error percentages are shown in Table 2. Fig. 4 and Table 2 both indicated the same result as Kuo et al. (2011): BCV is obviously the most accurate and stable extrapolation in Taiwan. The error percentages of STS and BCV are similar at the assumed depth of 15 m; however, BCV is definitely superior to STS at the greater depths. The lower standard deviations exhibited by BCV confirm that it is also the most stable extrapolation. BCV was again demonstrated to be the most accurate method owing to it producing the least discrepancies at all assumed depths; in addition, it generally resulted in a lower value of Vs30 to yield a more conservative result that is more appropriate for engineering applications (Boore, 2004). The Vs30 values of the 54 stations with velocity profiles less than 30 m were therefore derived using the BCV method in this study.

4. Empirical equations of S-wave velocity

Many empirical S-wave velocity equations, which were the relations established among soil indexes, have been evaluated in terms of their efficiency and economy (e.g., Ohsaki and Iwasaki, 1973; Ohta and Goto, 1978; Seed and Idriss, 1981; Lee, 1992; Japan Road

Fig. 4. Estimated Vs30 values (y-axis) by three extrapolation methods versus real Vs30 values (x-axis) obtained by PS-logging measurements in 385 stations with velocity profiles reaching at least 30 m. The assumed depths of 15, 20, and 25 m are represented as blue circles, black squares, and magenta diamonds, respectively.

Table 2
The percentage error obtained by extrapolation at three assumed depths from 385 boreholes reaching at least 30 m in Taiwan. The percentages behind "±" are the standard deviations.

Assumed depth (m)	Err% of 385 boreholes		
	LSS	STS	BCV
15	11.24 ± 8.16	6.98 ± 6.22	6.60 ± 5.65
20	8.03 ± 6.21	4.39 ± 3.76	3.06 ± 2.83
25	5.66 ± 4.45	2.05 ± 1.79	1.15 ± 1.24

Association, 2002; Chen et al., 2003; Lee and Tsai, 2008; Akin et al., 2011). Ohta and Goto (1978) first proposed a technique of multivariable analysis for empirical S-wave velocity equations. Kuo et al. (2011) consulted 13 representative studies and then proposed a procedure for evaluating the empirical equations for the Taipei Basin and the Ilan County. However, we think the procedure is too complex for the objects of the present study, which covers all seven regions of Taiwan, and a modified procedure was adopted. For example, the unified power-law regression model was used in all regions, and the soil types were categorized as sands (consisting of SC, SP, SM, and SW) and clays (consisting of CL, ML, CH, and MH), while the numbers of each soil type are greater than 100. In order to avoid the multicollinearity of the multivariable regression, which can be caused by two or more highly correlated independent variables, the present study adopted two examinations, the rule of thumb test and stepwise selection. We assumed that the two examinations can exclude one independent variable while the coupling of depth and the N value is too large to affect the regression result. The criteria of the examinations were suggested by Kuo et al. (2011). For the rule of thumb test, the correlation coefficient of two independent variables should be smaller than 0.7 (Anderson et al., 1984); for the stepwise selection, the probability of F had to be statistically lower than 0.05 for entry and higher than 0.1 for removal (Hair et al., 2006). In this way, the evaluated empirical S-wave velocity equations can be used to convert N profiles to S-wave velocity profiles without overburden-correction.

The purpose of the evaluated empirical equations is to estimate the S-wave velocities within the top 30 m of soil. Considering most of the drilled stations are less than 35 m and in order to reduce the influence of minority data at greater depths, the depths and N values of the data we select must be smaller than 35 m and 50, respectively. The codes of the TSMIP stations were assigned according to the abbreviations of the different regions of Taiwan Island, which are TAP, TCU, CHY, KAU, TTN, HWA, and ILA, counterclockwise from the north, as shown in Fig. 1. The empirical equations in the seven regions were evaluated in the present study. Although Kuo et al. (2011) had evaluated the empirical equations in TAP and ILA, we evaluated new ones in the present study due to the acquisition of several new drilled stations and the reduction of the depth criterion for data collection. Nevertheless, we only selected the data inside the Taipei Basin because the geological epochs are more complex in TAP (Kuo et al., 2011) and most of the soil sites are inside the basin.

The evaluated empirical equations, the standard deviations of the estimated S-wave velocities, and sample numbers used are shown in Table 3. It should be noted that the equations can only be applied to the strata of depth less than 35 m and the N values should be smaller than 50 due to the nature of the data collection. The data of TCU, HWA, the clays of ILA, and the sands of Taiwan passed the rule of thumb test, but failed in stepwise selection, due to the high coupling between two independent variables, that is the so-called multicollinearity, so we would not implement the multivariable regression for this data. The data sets in HWA and TTN will be less than 100 if we consider the soil types, so that all data sets of different soils were used together to assure rationality of the regression. The evaluated empirical S-wave velocity equations were plotted together in Fig. 5 as a function

Table 3
Evaluated empirical S-wave velocity equations in seven regions and the whole of Taiwan. The σ column shows the standard deviations of the calculated S-wave velocities.

| Region	Empirical Vs equation	σ	Soil type	Samples
CHY	$Vs = 114.29\, N^{0.130} D^{0.133}$	43.03	Sand	723
	$Vs = 114.02\, N^{0.115} D^{0.159}$	44.48	Clay	686
HWA	$Vs = 219.79\, N^{0.159}$	87.62	All	166
ILA	$Vs = 142.23\, N^{0.165} D^{0.05}$	46.39	Sand	327
	$Vs = 139.64\, N^{0.208}$	45.48	Clay	267
KAU	$Vs = 112.46\, N^{0.194} D^{0.118}$	65.09	Sand	380
	$Vs = 131.52\, N^{0.129} D^{0.113}$	50.61	Clay	330
TAP	$Vs = 99.08\, N^{0.233} D^{0.121}$	76.33	Sand	219
	$Vs = 118.03\, N^{0.156} D^{0.137}$	53.62	Clay	479
TCU	$Vs = 138.36\, N^{0.220}$	78.90	Sand	250
	$Vs = 172.98\, N^{0.207}$	88.24	Clay	202
TTN	$Vs = 233.35\, N^{0.171} D^{0.088}$	102.37	All	48
Taiwan	$Vs = 127.35\, N^{0.245}$	77.46	Sand	1645
	$Vs = 129.12\, N^{0.200} D^{0.065}$	67.38	Clay	1728

of N and at an assumed depth of 15 m for comparison. Those in TTN, HWA, and the clays of TCU are obviously larger than the others, which are spread across almost all of a zone.

5. Site classification of the drilled free-field TSMIP stations

Site classifications for the 439 drilled free-field TSMIP stations were achieved according to the Vs30 criteria of NEHRP (BSSC, 2001). The Vs30 was estimated by the BCV method for the 54 stations with velocity profiles less than 30 m. The classification and distribution are illustrated in Fig. 6. The yellow inverted triangle, indigo diamonds, blue squares, green triangles, and magenta circles denote Class A, B, C, D, and E, respectively. There are one site of Class A, 29 sites of Class B, 200 sites of Class C, 193 sites of Class D, and 16 sites of Class E. In Taiwan, most drilled stations belong to Class C and D (89.5%); this might be attributed to the fact that most of the stations were installed in metropolitan districts, which are usually located on sediments or soft rocks. The others account for only 10.5%. Stations of Class D and E are mainly distributed on plains and basins with unconsolidated sediments, those of Class C are located on the northwestern part of Taiwan and around the Central Mountain and the Coastal Range, those of Class B are mostly located on the north and south of Taiwan and several are in mountain areas, and the unique Class A in
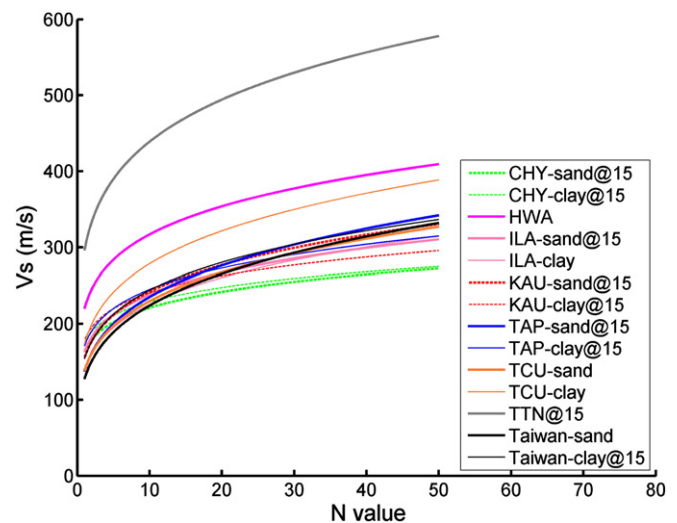
Fig. 5. Empirical S-wave velocity equations for different regions and for the whole of Taiwan. The marker "@15" indicates that the curves are at a depth of 15 m for the comparison. As shown in the legend, thick curves represent sands or all soils; thin curves represent clays.
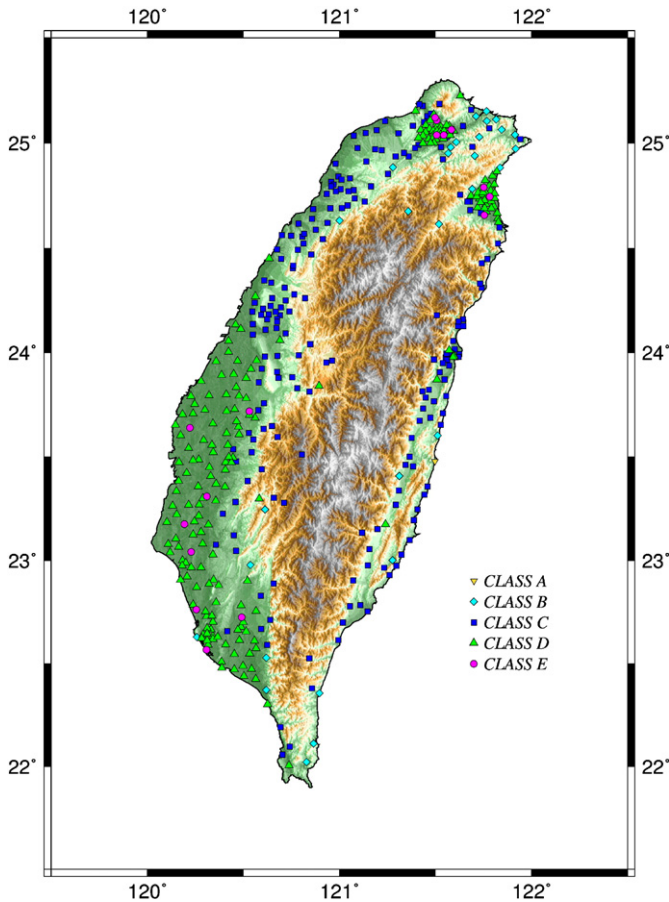
Fig. 6. Site classification and locations of the 439 drilled free-field TSMIP stations in Taiwan. The yellow inverted triangle, indigo diamonds, blue squares, green triangles, and magenta circles denote Class A, B, C, D, and E sites, respectively.

the database is on the Coastal Range. Site classification and the measured Vs30 of the present study are listed in Table A1. These significant results are important reference materials for the NGA studies that are prevalent in modern research.

6. Discussions

The cooperative drilling project is still under implementation. The earthquake catalogs of the stations where boreholes have not yet been drilled will be inspected to find those which recorded more earthquake events or exhibited notable site responses, and then the drilling objectives for following years will be determined. A number of studies which were provided with beneficial information from the EGDT were published. For example, Huang et al. (2007, 2009) used the logging data in central Taiwan and in the Taipei Basin to estimate the high frequency site amplification by using the quarter-wavelength method. Sokolov et al. (2007) referred to the peculiarity of the H/V ratios at TAP051, which was classified as class B by Lee et al. (2001); however, the measured Vs30 is only 401.82 m/s. It was reclassified into the class C2 (its Vs30 is between 490 and 620 m/s) by Lee and Tsai (2008), but the result was still not reliable. Kuo et al. (2009) used several S-wave velocity profiles at Ilan of EGDT to test the feasibility of investigating shallow S-wave velocity structures using SASW and microtremor array techniques. In view of the fact that many organizations, such as the United States Geological Survey, the State University of New York, the Tokyo Institute of Technology, and the Karlsruhe University, had applied for EGDT data, but the

annual reports were written in Chinese, we therefore introduced the EGDT in this paper to help more users understand the database.

An accurate extrapolation allows for velocity profiles less than 30 m to be estimated. This method calculated Vs30 at 54 stations for EGDT and we are therefore convinced it can help in estimating Vs30 values at other boreholes less than 30 m. After comparison, BCV was demonstrated to be the most accurate extrapolation for use in Taiwan; on the other hand, Boore (2004) indicated that the STS is the most accurate method for use in California. Kuo et al. (2011) compared average S-wave slowness at different depths and found that the S-wave velocities increase more slowly in northeastern Taiwan than in California on the average. We speculate that the same phenomenon would be found for the whole of Taiwan. The reason why the average S-wave velocities increase more gently in Taiwan is beyond the scope of this paper.

We evaluated the empirical S-wave velocity equations for the seven regions and the whole of Taiwan in this study in order to make the conversion of N profiles to S-wave velocity profiles more easy and accurate. The S-wave velocities measured by a PS-logger system were calculated by identifying the first arrivals of two receivers at a depth; by contrast, the S-wave velocities measured by tra-ditional down-hole or up-hole methods were calculated from slopes of travel times at several continuous depths, so that the velocity was iden-tical during a section of the depth but different N values might be obtained in this section. In other words, most of the measured N values of the EGDT also have S-wave velocities at the corresponding depths, so that the data of the EGDT is more suitable for evaluating empirical S-wave velocity equations.

In addition we adopted the rule of thumb test and stepwise selec-tion to examine the collected data before the regression to avoid the strong coupling between depth and N. It is valid to assume that the coupling of N and depth is negligible in those regions which the data pass both the tests. The evaluated empirical equations in TTN, HWA, and the clays of TCU are larger than others (Fig. 5). This phe-nomenon seems to reflect the general sense of the geological back-ground of Taiwan (Ho, 1975). The site classification in Fig. 6 also showed that the class C stations are mainly located in the HWA, TTN, and TCU regions. The purpose of evaluating the empirical equa-tions is that many existing engineering boreholes in Taiwan only have N profiles but no velocity profiles. We believe the proposed empirical equations and extrapolation can be used together for those boreholes, and thus the S-wave velocity profile can be derived by the empirical equations. Moreover, for some of those with depths less than 30 m, Vs30 can then be estimated by the extrapolation. Two examples of the practical application can be found in Kuo et al. (2011).

The major objective of this study was to reclassify the free-field TSMIP stations and calculate the Vs30 values. Table A1 tabulates the coordinates and site classifications of the 439 free-field TSMIP sta-tions considered in this paper, and by Lee et al. (2001), Phung et al. (2006), and Lee and Tsai (2008), as well as the measured and estimat-ed Vs30 values. Based on the site classification adopted in this study, it was found that 276 of the 419 mutual stations were misclassified by Lee et al. (2001), 96 of the 278 mutual stations were misclassified by Phung et al. (2006), and 80 of the 436 stations in common were mis-classified by Lee and Tsai (2008). The site classification of Lee et al. (2001) is still the most widely-used classification; however, our re-sult shows that over 60% of the mutual stations were misclassified due to lack of site-specific information. Phung et al. (2006) only classified the sites as soil and rock, so the rate of misclassification seems lower. A recently revised classification proposed by Lee and Tsai (2008) was much more accurate than the previous version. They used the logging data of 257 stations in the EGDT, and the rate of misclassified stations was less than 20% as a result.

However, Vs30 values are also the critical parameter for recent studies of ground motion prediction models. Fig. 7 showed large divergences between the measured Vs30 (x-axis) by PS-logging and
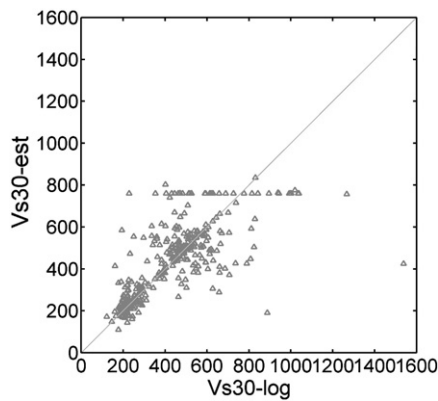
Fig. 7. Comparison of the estimated Vs30 (*y*-axis) by Lee and Tsai (2008) and the measured Vs30 (*x*-axis) by a Suspension PS Logger system. The estimated Vs30 values were obviously limited to around the boundary of Class B and C in their estimation.

the estimated Vs30 (*y*-axis) of Lee and Tsai (2008) at the 382 mutual stations with velocity profiles reaching at least 30 m. Their estimated Vs30 clearly lose accuracy near and above the boundary of B and C, so that the concentration near the boundary was generated. In fact, the maximum Vs30 of their estimation was 835 m/s at TAP071. The Vs30 of a group of 99 stations was estimated to be 760 m/s. Of these, 95 were classified Class B, but the other four were classified Class C for an unknown reason. We quantified the deviations within Fig. 7 by Eq. (3), and thus the percentage error is 18.6%. After further considering that they used the data of the EGDT obtained in 2000 to 2005, we calculated the percentage error in this period and in 2006 to 2010. The error percentages, which are 12.9% and 26.8% in the two periods, indicate that the accuracy of the estimated Vs30 is obviously lower for the unknown stations. The above descriptions imply that the accuracy of site classification and Vs30 estimation increased after the logging data were utilized; however, due to the complex near-surface geological conditions in Taiwan, we still need more logging data to further investigate the detailed site effects at those uncharacterized sites.

7. Conclusions

It was considered essential to understand the variable geological conditions at strong motion stations, in order to assess the site effects more exactly. A lengthy drilling project on free-field TSMIP stations was therefore conducted cooperatively by the NCREE and the CWB to construct the EGDT. The EGDT is comprised of coordinates of stations and boreholes, sketches, photographs, and descriptions of surrounding environment, and locations marked on aerial photographs; as well, the physical characteristics and categories of soils, N values, and P- and S-wave velocity profiles were included. This paper provided a set of specifications and a description to help users understand the subject matter, and then calculated the Vs30 as well as the site classification of all drilled stations.

In view of the fact that the strong motion recordings from the Chi-Chi earthquake were included in the NGA's database, their precise site classification and the Vs30 values of free-field TSMIP stations are essential for strong motion predictions. A total of 54 of the 439 drilled stations have velocity profiles less than 30 m in the EGDT. This paper examined three common extrapolations, i.e., LSS, STS, and BCV, using those velocity profiles greater than or equal 30 m at three assumed depths. BCV was shown to be the most accurate and stable extrapolation because it had the least error percentages and standard deviations at all assumed depths. The Vs30 values of the 54 stations were therefore estimated using BCV in this study. Additionally, the empirical S-wave velocity equations at the seven regions and which for the whole of Taiwan were evaluated. The data were examined by the rule of thumb test and stepwise selection before

the multivariable regression to avoid strong coupling between depth and N. For the data passed both the tests, we then evaluated the correlations of S-wave velocities, blow numbers, and depth for the regions; however, for those data did not passed the tests, we only evaluated the correlations between S-wave velocities and N due to the non-negligible coupling in those regions. The evaluated empirical equations seem to reflect the nature of geological conditions in Taiwan, that the near-surface velocities in TTN, HWA, and TCU are larger than in other regions (Fig. 5). The site classification (Fig. 6) showed this as well. The main motive in evaluating the empirical equations was that many existing engineering boreholes in Taiwan only had N profiles but no velocity profiles; of course, many of them were shallower than 30 m. The proposed empirical equations and extrapolation of Vs30 can be used together to estimate S-wave velocity profiles and Vs30 for those boreholes without additional expense. We are convinced that this approach can help us to develop more detailed and accurate investigations of Vs30 in the future.

The Vs30 of 439 drilled stations were calculated and then the site classification was achieved according to the NEHRP's Vs30 criteria. The results are shown in Fig. 6 and Table A1. The accuracy of the modified classification (Lee and Tsai, 2008), which used 257 stations of EGDT (drilled during 2000 to 2005) and another 4885 engineering boreholes, were indeed improved over the previous result (Lee et al., 2001). However, after quantification of the discrepancy, the error percentage was shown to be 18.6%. Furthermore, the error percentages are 12.9% and 26.8% during 2000 to 2005 and 2006 to 2010. This indicates that the errors of the estimated Vs30, which were obtained afterwards, must be larger than those given. Another ambiguity was that the Vs30 of 99 stations was estimated at an identical value of 760 m/s, but 95 of them were classified Class B and the others were classified Class C. We have shown that the accuracy of the site classification and Vs30 estimates in this study is much better than in previous studies; however, the number of drilled stations is still not enough. It is believed that the continued drilling project and the employment of empirical S-wave velocity equations and Vs30 extrapolation will increase the number of applicable Vs30 values in future years.

Appendix A. Supplementary data

Supplementary data to this article can be found online at doi:10.1016/j.enggeo.2012.01.013.

References

Akin, M.K., Kramer, S.L., Topal, T., 2011. Empirical correlations of shear wave velocity (Vs) and penetration resistance (SPT-N) for different soils in an earthquake-prone area (Erbaa-Turkey). Engineering Geology 119, 1–17.

Anderson, D.R., Sweeney, D.J., Williams, T.A., 1984. Statistics for business and economics, second edition. West publishing Company, Taipei.

Boore, D.M., 2003. A compendium of P- and S-wave velocities from surface-to-borehole logging: summary and reanalysis of previously published data and analysis of unpublished data. U.S. Geological Survey Open-File Report 03-191.

Boore, D.M., 2004. Estimating Vs(30) (or NEHRP site classes) from shallow velocity models (Depths <30 m). Bulletin of the Seismological Society of America 94 (2), 591–597.

Boore, D.M., Joyner, W.B., 1997. Site amplifications for generic rock sites. Bulletin of the Seismological Society of America 87 (2), 327–341.

Building Seismic Safety Council (BSSC), 2001. NEHRP recommended provisions for seismic regulations for new buildings and other structures, Part 1: Provisions, prepared by the Building Seismic Safety Council for the Federal Emergency Management Agency (Report FEMA 368), Washington, D.C., 2000 Edition.

Campbell, S.W., Bozorgnia, Y., 2008. NGA ground motion model for the geometric mean horizontal component of PGA, PGA, PGD and 5% damped linear elastic response spectra for periods ranging from 0.01 to 10 s. Earthquake Spectra 24, 139–171.

Chen, M.H., Wen, K.L., Loh, C.H., 2003. A study of shear wave velocities for alluvium deposits in southwestern Taiwan. Journal of Chinese Institute of Civil and Hydraulic Engineering 15 (4), 667–677.

Chiou, B.S.J., Youngs, R.R., 2008. An NGA model for the average horizontal component of peak ground motion and response spectra. Earthquake Spectra 24, 173–215.

Chiou, B.S.J., Darragh, R., Gregor, N., Silvad, W., 2008. NGA project strong motion database. Earthquake Spectra 24 (1), 23–44.

Dobry, R., Borcherdt, R.D., Crouse, C.B., Idriss, I.M., Joyner, W.B., Martin, G.R., Power, M.S., Rinne, E.E., Seed, R.B., 2000. New site coefficients and site classification system used in recent building seismic code provisions. Earthquake Spectra 16, 41–67.

Hair, J.J.F., William, C.B., Barry, J.B., Rolph, E.A., Ronald, L.T., 2006. Multivariate data analysis, 6th edition. Pearson Education International, Upper Saddle River. NJ.

Ho, C.S., 1975. An introduction to the geology of Taiwan, explanatory text of the geologic map of Taiwan. Ministry of Economic Affairs, Republic of China.

Holzer, T.L., Bennett, M.J., Noce, T.E., Padovani, A.C., Tinsley III, J.C., 2002. Liquefaction hazard and shaking amplification maps of Alameda, Berkeley, Emeryville, Oakland and Piedmont, California: a digital database. U.S. Geological Survey Open-File Report, 02-296.

Holzer, T.L., Bennett, M.J., Noce, T.E., Padovani, A.C., Tinsley, J.C.I.I.I., 2005. Shear-wave velocity of surficial geologic sediments in northern California: statistical distributions and depth dependence. Earthquake Spectra 21 (1), 161–177.

Huang, M.W., Wang, J.H., Ma, K.F., Wang, C.Y., Hung, J.H., Wen, K.L., 2007. Frequency-dependent site amplifications with f ≧ 0.01 Hz evaluated from velocity and density models in central Taiwan. Bulletin of the Seismological Society of America 97 (2), 624–637.

Huang, M.W., Wang, J.H., Hsieh, H.H., Wen, K.L., 2009. High frequency site amplification evaluated from Borehole data in the Taipei Basin. Journal of Seismology 13 (4), 601–611.

Japan Road Association, 2002. Specification for Highway Bridges, Part V: Seismic Design. Tokyo, Japan.

Koppes, M.N., Montgomery, D.R., 2009. The relative efficacy of fluvial and glacial erosion over modern to orogenic timescales. Nature Geoscience 2, 644–647.

Kuo, C.H., Cheng, D.S., Hsieh, H.H., Chang, T.M., Chiang, H.J., Lin, C.M., Wen, K.L., 2009. Comparison of three different methods in investigating shallow shear-wave velocity structures in Ilan, Taiwan. Soil Dynamics and Earthquake Engineering 29 (1), 133–143.

Kuo, C.H., Wen, K.L., Hsieh, H.H., Chang, T.M., Lin, C.M., Chen, C.T., 2011. Evaluating empirical regression equations for Vs and estimating Vs30 in northeastern Taiwan. Soil Dynamics and Earthquake Engineering 31 (3), 431–439.

Lee, S.H.H., 1992. Analysis of the multicollinearity of regression equations of shear wave velocities. Soils and Foundations 32 (1), 205–214.

Lee, C.T., Tsai, B.R., 2008. Mapping Vs30 in Taiwan. Terrestrial, Atmospheric and Oceanic Sciences 19 (6), 671–682.

Lee, C.T., Cheng, C.T., Liao, C.W., Tsai, Y.B., 2001. Site classification of Taiwan free-field strong-motion stations. Bulletin of the Seismological Society of America 91 (5), 1283–1297.

Liew, P.M., Pirazzoli, P.A., Hsieh, M.L., Arnold, M., Barusseau, J.P., Fontugne, M., Giresse, P., 1993. Holocene Tectonic Uplift Deduced from Elevated Shorelines, Eastern Coastal Range of Taiwan. Tectonophysics 222, 55–68.

Ohsaki, Y., Iwasaki, R., 1973. On dynamic shear moduli and Poisson's ratio of soil deposits. Soils and Foundations 13 (4), 61–73.

Ohta, Y., Goto, N., 1978. Empirical shear wave velocity equations in terms of characteristic soil indexes. Earthquake Engineering and Structural Dynamics 6, 167–187.

OYO Corporation, 1999. Operation Manual, Model-3915/3954, Type 350 Winch. Tsukuba Technical Research and Development Center, Japan.

OYO Corporation, 2000. Operation Manual, Model-3302A, Suspension PS Logging Probe (for 4 – conductor armored cable). Tsukuba Technical Research and Development Center, Japan.

OYO Corporation, 2002. Operation Manual, Model-3660A, Suspension PS Logger. Tsukuba Technical Research and Development Center, Japan.

Phung, V., Atkinson, G.M., Lau, D.T., 2006. Methodology for site classification estimation using strong ground motion data from the Chi-Chi, Taiwan, Earthquake. Earthquake Spectra 22, 511–531.

Power, M., Chiou, B., Abrahamson, N., Bozorgnia, Y., Shantz, T., Roblee, C., 2008. An overview of the NGA project. Earthquake Spectra 24 (1), 3–21.

Seed, H.B., Idriss, I.M., 1981. Evaluation of liquefaction potential of sand deposits based on observations of performance in previous earthquakes. Proceedings of the Conference on In Situ Testing to Evaluate Liquefaction Susceptibility, ASCE, pp. 81–544.

Sino Geotechnology, Inc., 2002-2010. Record Report of Drilling and Investigation at Strong Motion Stations. National Center for Research on Earthquake Engineering. (In Chinese).

Sokolov, V.Y., Loh, C.H., Jean, W.Y., 2007. Application of horizontal-to-vertical (H/V) Fourier spectral ratio for analysis of site effect on rock (NEHRP-class B) sites in Taiwan. Soil Dynamics and Earthquake Engineering 27 (4), 314–323.

Wen, K.L., Lin, C.M., Chiang, H.J., Kuo, C.H., Huang, Y.C., Pu, H.C., 2008. Effect of Surface Geology on Ground Motions: the Case of TAP056. Terrestrial, Atmospheric and Oceanic Sciences 19, 451–462.